

Electrophysiology

Mice were used at 4–8 weeks old. Local field potentials (EVG) were recorded from the luminal surface of intact VNO sensory epithelia⁹. 2,5-dimethylpyrazine, 2-heptanone, *n*-pentyl acetate and isobutylamine were purchased from Aldrich; 2-*sec*-butyl-4,5-dihydrothiazole from Alfa Aesar; and farnesene from Bedoukian Research.

Received 24 January; accepted 20 June 2002; doi:10.1038/nature00955.

1. Halpern, M. The organisation and function of the vomeronasal system. *Annu. Rev. Neurosci.* **10**, 325–362 (1987).
2. Keverne, E. B. The vomeronasal organ. *Science* **286**, 716–720 (1999).
3. Dulac, C. & Axel, R. A novel family of genes encoding putative pheromone receptors in mammals. *Cell* **83**, 195–206 (1995).
4. Tirindelli, R., Mucignat-Caretta, C. & Ryba, N. J. Molecular aspects of pheromonal communication via the vomeronasal organ of mammals. *Trends Neurosci.* **21**, 482–486 (1998).
5. Ramirez-Solis, R., Liu, P. & Bradley, A. Chromosome engineering in mice. *Nature* **378**, 720–724 (1995).
6. Del Punta, K., Rothman, A., Rodriguez, I. & Mombaerts, P. Sequence diversity and genomic organization of vomeronasal receptor genes in the mouse. *Genome Res.* **10**, 1958–1967 (2000).
7. Rodriguez, I., Del Punta, K., Rothman, A., Ishii, T. & Mombaerts, P. Multiple new and isolated families within the mouse superfamily of V1r vomeronasal receptors. *Nature Neurosci.* **5**, 134–139 (2002).
8. Holy, T. E., Dulac, C. & Meister, M. Responses of vomeronasal neurons to natural stimuli. *Science* **289**, 1569–1572 (2000).
9. Leinders-Zufall, T. *et al.* Ultrasensitive pheromone detection by mammalian vomeronasal neurons. *Nature* **405**, 792–796 (2000).
10. Sam, M. *et al.* Odorants may arouse instinctive behaviours. *Nature* **412**, 142 (2001).
11. Wysocki, C. J. & Lepri, J. J. Consequences of removing the vomeronasal organ. *J. Steroid Biochem. Mol. Biol.* **4**, 661–669 (1991).
12. Lane, R. P., Cutforth, T., Axel, R., Hood, L. & Trask, B. J. Sequence analysis of mouse vomeronasal receptor gene clusters reveals common promoter motifs and a history of recent expansion. *Proc. Natl Acad. Sci. USA* **99**, 291–296 (2002).
13. Bean, N. J. & Wysocki, C. J. Vomeronasal organ removal and female mouse aggression: the role of experience. *Physiol. Behav.* **45**, 875–882 (1989).
14. Bean, N. J. Olfactory and vomeronasal mediation of ultrasonic vocalizations in male mice. *Physiol. Behav.* **28**, 31–37 (1982).
15. Wysocki, C. J., Nyby, J., Whitney, G., Beauchamp, G. K. & Katz, Y. The vomeronasal organ: primary role in mouse chemosensory gender recognition. *Physiol. Behav.* **29**, 315–327 (1982).
16. Bean, N. J. Modulation of agonistic behavior by the dual olfactory system in male mice. *Physiol. Behav.* **29**, 433–437 (1982).
17. Clancy, A. N., Coquelin, A., Macrides, F., Gorski, R. A. & Noble, E. P. Sexual behavior and aggression in male mice: involvement of the vomeronasal system. *J. Neurosci.* **4**, 2222–2229 (1984).
18. Ogawa, S. *et al.* Abolition of male sexual behaviors in mice lacking estrogen receptors α and β ($\alpha\beta$ ERKO). *Proc. Natl Acad. Sci. USA* **97**, 14737–14741 (2000).
19. Amoore, J. E. & Steinle, S. In *Chemical Senses* Vol. 3, *Genetics of Perception and Communication* (eds Wysocki, C. J. & Klare, M. R.) 331–351 (Marcel Dekker, New York, 1991).
20. Takigami, S. *et al.* The expressed localisation of rat putative pheromone receptors. *Neurosci. Lett.* **272**, 115–118 (1999).
21. Belluscio, L., Koentges, G., Axel, R. & Dulac, C. A map of pheromone receptor activation in the mammalian brain. *Cell* **97**, 209–220 (1999).
22. Rodriguez, I., Feinstein, P. & Mombaerts, P. Variable patterns of axonal projections of sensory neurons in the mouse vomeronasal system. *Cell* **97**, 199–208 (1999).
23. Mombaerts, P. Seven-transmembrane proteins as odorant and chemosensory receptors. *Science* **286**, 707–711 (1999).
24. Firestein, S. How the olfactory system makes sense of scents. *Nature* **413**, 211–218 (2001).
25. Slotnick, B. & Bodyak, N. Odor discrimination and odor quality perception in rats with disruption of connections between the olfactory epithelium and olfactory bulbs. *J. Neurosci.* **22**, 4205–4216 (2002).
26. Hildebrand, J. G. Analysis of chemical signals by nervous systems. *Proc. Natl Acad. Sci. USA* **92**, 67–74 (1995).
27. Sorensen, P. W., Christensen, T. A. & Stacey, N. E. Discrimination of pheromonal cues in fish: emerging parallels with insects. *Curr. Opin. Neurobiol.* **8**, 458–467 (1998).
28. Leybold, B. G. *et al.* Altered sexual and social behaviors in *trp2* mutant mice. *Proc. Natl Acad. Sci. USA* **99**, 6376–6381 (2002).
29. Stowers, L., Holy, T. E., Meister, M., Dulac, C. & Koentges, G. Loss of sex discrimination and male aggression in mice deficient for TRP2. *Science* **295**, 1493–1500 (2002).
30. Matzuk, M. M., Finegold, M. J., Su, J. G., Hsueh, A. J. & Bradley, A. Alpha-inhibin is a tumour-suppressor gene with gonadal specificity in mice. *Nature* **360**, 313–319 (1992).

Acknowledgements

We thank R. Peraza and A. Walsh for producing chimaeric mice, D. Pfaff for fostering this collaboration, M. Novotny for providing 2,3-dehydro-*exo*-brevicommin and 6-hydroxy-6-methyl-3-heptanone, and T. Bozza, S. Firestein, C. Greer, K. Kelliher and D. Pfaff for critical reading of the manuscript. Postdoctoral fellowship support to I.R. was from the Swiss National Foundation for Research. Grant support to T.L.-Z. and F.Z. was from NIH/NIDCD, and to P.M. from the March of Dimes Birth Defects Foundation.

Competing interests statement

The authors declare that they have no competing financial interests.

Correspondence and requests for materials should be addressed to P.M. (e-mail: peter@rockefeller.edu).

The *ELF4* gene controls circadian rhythms and flowering time in *Arabidopsis thaliana*

Mark R. Doyle^{*†}, Seth J. Davis^{†‡}, Ruth M. Bastow^{‡§}, Harriet G. McWatters[‡], László Kozma-Bognár^{||}, Ferenc Nagy^{||}, Andrew J. Millar[‡] & Richard M. Amasino^{*}

^{*} Department of Biochemistry and Program in Cellular and Molecular Biology, University of Wisconsin-Madison, Madison, Wisconsin 53706, USA

[‡] Department of Biological Sciences, University of Warwick, Coventry CV4 7AL, UK

^{||} Institute of Plant Biology, Biological Research Center, H-6726 Szeged, Hungary

[†] These authors contributed equally to this work

[§] Present address: John Innes Centre, Norwich NR4 7UH, UK

Many plants use day length as an environmental cue to ensure proper timing of the switch from vegetative to reproductive growth. Day-length sensing involves an interaction between the relative length of day and night, and endogenous rhythms that are controlled by the plant circadian clock¹. Thus, plants with defects in circadian regulation cannot properly regulate the timing of the floral transition². Here we describe the gene *EARLY FLOWERING 4* (*ELF4*), which is involved in photoperiod perception and circadian regulation. *ELF4* promotes clock accuracy and is required for sustained rhythms in the absence of daily light/dark cycles. *elf4* mutants show attenuated expression of *CIRCADIAN CLOCK ASSOCIATED 1* (*CCA1*), a gene that is thought to function as a central oscillator component^{3,4}. In addition, *elf4* plants transiently show output rhythms with highly variable period lengths before becoming arrhythmic. Mutations in *elf4* result in early flowering in non-inductive photoperiods, which is probably caused by elevated amounts of *CONSTANS* (*CO*), a gene that promotes floral induction⁵.

In *Arabidopsis*, a facultative long-day plant, the floral transition occurs earlier when plants are grown in long days (LD) than when they are grown in short days (SD)⁶. *elf4* mutants flower early in SD and are therefore impaired in their ability to sense day length (Table 1). In addition, *elf4* mutants have elongated hypocotyls and petioles (Table 1), particularly in SD. Both of these phenotypes may result from defects in circadian regulation^{7,8}. A hallmark of circadian regulation is the persistence of robust, accurate rhythms for many days under conditions of continuous light (LL) or continuous darkness (DD). Circadian outputs, including rhythmic leaf movements and the expression of chlorophyll *a/b*-binding protein (*CAB*) and cold- and circadian-regulated (*CCR*) genes, are markers of clock function.

We introduced the luciferase reporter gene fusions *CAB-LUC* and *CCR2-LUC* into wild-type and *elf4* mutant plants. *CAB* rhythms in wild-type persisted in LL, whereas *elf4* mutants lost rhythmicity after one 24-h cycle (Fig. 1a). The arrhythmicity of the

Table 1 Flowering time and hypocotyl lengths of *elf4* mutants

	Total leaf number*		Hypocotyl length (mm)†		
	LD	SD	CL	LD	SD
Wild type	7.8 ± 0.4 (30)	30.6 ± 5.1 (28)	2.9 ± 0.7	2.2 ± 0.7	4.7 ± 1.3
<i>elf4</i>	6.4 ± 0.9 (36)	10.1 ± 1.1 (23)	2.4 ± 0.4	3.1 ± 0.7	9.0 ± 1.9
<i>elf3-4</i>	4.9 ± 0.3 (36)	5.9 ± 0.3 (23)	2.8 ± 0.6	6.0 ± 0.2	10.2 ± 2.2

* Mean ± s.d. total leaf number was counted as rosette leaves plus cauline leaves. The number of plants is given in parentheses.

† About 15 plants were analysed in each trial.

CL, continuous light; LD, 16 h light/8 h dark; SD, 8 h light/16 h dark.

population (Fig. 1a) concealed weak rhythms of variable period in individual *elf4* seedlings: many *elf4* seedlings had shorter or longer periods than those of wild-type seedlings (Fig. 1b). Unlike *CAB-LUC*, *CCR2-LUC* maintains a robust pattern of expression in DD. *elf4* seedlings showed weak *CCR2* expression rhythms of variable period in DD (Fig. 1d), which, like *CAB*, seemed arrhythmic in the population mean (Fig. 1c). Expression of *CCR2* also had variable periods in individual seedlings in LL (data not shown). For each marker, the rhythms of individual *elf4* seedlings damped before the rhythms of wild-type seedlings (data not shown).

Leaves of *Arabidopsis* show circadian movements that result in a

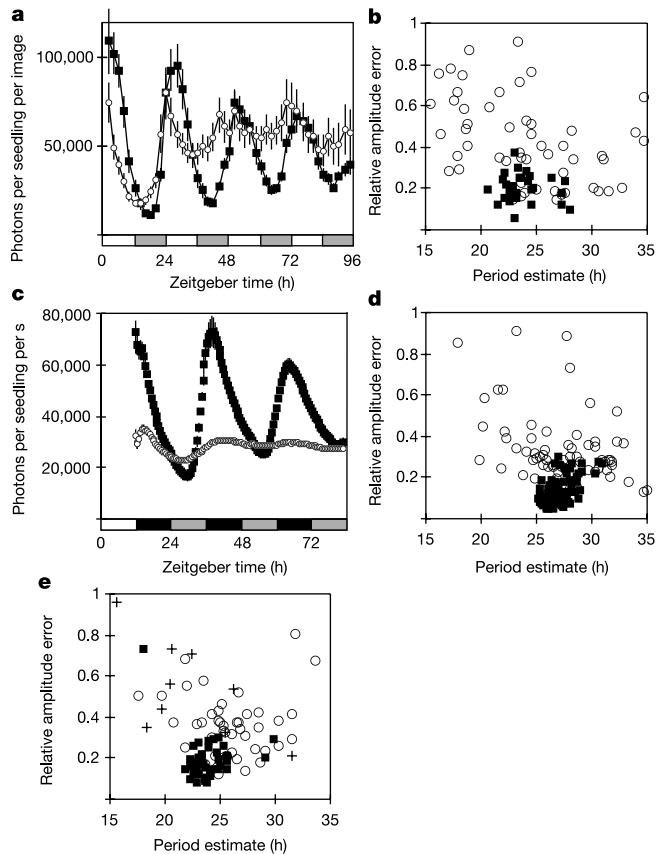


Figure 1 Circadian rhythms of *elf4* in LL or DD. **a**, *CAB-LUC* activity in plants transferred to LL at 0 h (predicted dawn). The transgene was crossed into *elf4*. Data are the means \pm s.e.m. of eight individual seedling traces. **b**, *CAB-LUC* activity in LL in individual seedlings. The period estimate for each seedling is plotted against the relative amplitude error, a measure of rhythmic robustness that varies from 0 (a perfect cosine wave) to 1 (not statistically significant). Wild-type seedlings (30/30) were strongly rhythmic with a period of 23.8 ± 1.6 h (mean \pm s.d.), whereas *elf4* seedlings (55/71) were weakly rhythmic with a period of 22.3 ± 5.1 h. **c**, *CCR2-LUC* activity in plants transferred to DD at 12 h (predicted dusk). At least 40 plants per line were tested for three independently transformed wild-type lines and four *elf4* lines. Data are normalized to the genotype mean; error bars show the standard deviation of each line from the genotype mean. **d**, Analysis of *CCR2-LUC* activity in DD. Wild-type (87/87) and *elf4* seedlings (67/89) were rhythmic, with periods of 26.4 ± 0.8 h and 27.1 ± 4.1 h, respectively. **e**, Rhythmic leaf movement in LL. Wild-type (45/45) and *elf4* (50/60) traces were rhythmic, with periods of 25.1 ± 1.3 h and 25.9 ± 3.2 h, respectively. In *elf3*, only 9 out of 20 traces were rhythmic, with a period of 22.5 ± 4.8 h. Filled squares, wild type; open circles, *elf4*; plus signs, *elf3*. **a** and **c** are representative of two independent experiments; **b**, **d**, **e** show pooled data representing three, two and three experiments, respectively. Grey bars represent subjective day and subjective night in **a** and **c**, respectively.

horizontal position during the day and a more vertical position at night. A large percentage of *elf4* seedlings showed rhythmic leaf movements for the first 1–2 d in LL; however, these rhythms were less robust than in wild type and were no longer detectable after 3 d (Supplementary Information Fig. 1). Similar to gene expression studies, the period of leaf movement in *elf4* varied greatly among individuals (Fig. 1e). *ELF4* is therefore important for the maintenance and accuracy of circadian rhythms under LL and DD, as tested through different outputs.

Early flowering, hyperelongation and impaired circadian rhythms in LL are all characteristics of *elf3* mutants^{9,10}. In wild-type plants, *ELF3* sustains rhythmicity in long photoperiods and in LL by inhibiting phototransduction at dusk^{11–13}. In contrast to *elf4*, *CAB-LUC* and *CCR2-LUC* expression in *elf3* mutants resembles that of the wild type in DD^{13,14}. Also, *CAB-LUC* expression and leaf movement become arrhythmic immediately under LL in *elf3* mutants^{8,15}, rather than after one cycle as in *elf4* mutants (Fig. 1a). Thus, the function of *ELF4* is distinct from that of *ELF3*.

Although the *elf4* phenotype is unique in plants, the phenotype is similar to *frequency (frq)* mutants of *Neurospora crassa*. *Frq* participates in a rhythmic, transcriptional feedback loop that is essential for normal circadian rhythmicity¹⁶. Mutants that are null for *frq* can seem arrhythmic in constant conditions, but weak conidiation rhythms have been detected in these mutants, with periods that are distributed broadly about the wild-type mean¹⁷. This resembles the phenotype that we have shown for *elf4*. It is unclear whether *Frq* principally generates rhythms or organizes *Frq*-independent oscillators¹⁶. In an analogous fashion, *ELF4* could function in either process in the plant clock.

Arabidopsis genes that are thought to function in the circadian oscillator include *TIMING OF CAB EXPRESSION 1 (TOC1)*, which is expressed early in the night¹⁸, and *CCA1*, which is expressed

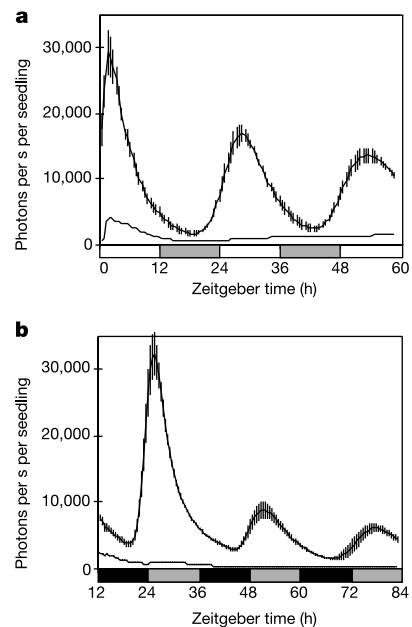


Figure 2 Regulation of *CCA1* expression by *ELF4*. Wild-type (line with error bars) and *elf4* (continuous line) plants containing a *CCA1-LUC* fusion assayed in LL (**a**) or DD (**b**). At least 18 plants per line in **a** or at least 40 plants per line in **b** were tested for five independently transformed wild-type and six *elf4* lines. *CCA1* expression was low in *elf4* (in LL: wild-type, $8,938 \pm 1,631$ counts per seedling per s (mean \pm s.e.m.); *elf4*, $1,330 \pm 478$; in DD: wild-type $7,178 \pm 927$; *elf4*, 613 ± 156). Data are normalized to the genotype mean and are representative of two independent experiments.

shortly after dawn⁴. The *elf4* lesion disrupted rhythmic *CCA1* expression, showing the importance of *ELF4* in circadian regulation. The expression of a *CCA1-LUC* reporter gene was low and arrhythmic in *elf4* seedlings under both LL and DD (Fig. 2). *CCA1* expression in *elf4* occurred only through acute light activation after the dark/light transition (Fig. 2a). This low amplitude pulse of *CCA1* might have supported the single cycle of *CAB-LUC* and *CCR2-LUC* expression in *elf4* in LL (Fig. 1a and data not shown), before the normal rhythm was lost around subjective dawn of the subsequent cycle, when *CCA1* was again required but was not expressed. We propose that the circadian function of *ELF4* is to activate light-inducible clock components around dawn: *CCA1* could be one such component. *TOC1* may carry out a similar activation function³.

elf4 was derived from a population mutagenized with the transfer DNA (tDNA) of *Agrobacterium tumefaciens*¹⁹. Adjacent to the tDNA was a deleted region predicted to contain a small open reading frame (ORF). A clone containing this ORF was sufficient to restore the phenotypes of *elf4* to that of wild type (Supplementary Information Fig. 2). In LL, the *ELF4* transcript maintains a robust rhythm, which shows that transcript abundance is under circadian control (Fig. 3a,

b). Robust cycling is not detectable after transfer to DD (Fig. 3a, c), which is similar to what has been observed for *TOC1* and *ELF3* (refs 12, 18). *ELF4* also shows a photoperiod-specific pattern of expression. In LD, messenger RNA levels peak around 12 h after dawn (Fig. 3d, e). In SD, the peak shifts to around 8 h after dawn (Fig. 3d, e). The predicted *ELF4* protein is 111 amino acids and does not contain known protein signatures (Supplementary Information Fig. 3). So far, organisms other than plants have not been found to contain genes similar to *ELF4*.

The circadian clock is thought to function in the floral transition through a coincidence mechanism in which inductive stimuli must be present during a particular phase of the rhythm to be effective¹. Given its strong effect on circadian outputs, *ELF4* could repress flowering by controlling the phase of an output rhythm specific for flowering-time regulation. The floral-promoting gene *CO* may act in such an output^{5,20,21}. The diurnal pattern of *CO* mRNA accumulation is distinct in inductive versus non-inductive photoperiods, and this expression pattern could contribute to a coincidence mechanism²¹. Several circadian rhythm mutants affect *CO* expression in ways that correlate with their early or late flowering phenotypes²¹. In SD-grown *elf4* mutants, the level of *CO* mRNA is increased at all time points (Fig. 3f, g). Increased *CO* expression is consistent with the early flowering *elf4* phenotype²¹.

The molecular circuitry that comprises the *Arabidopsis* circadian clock is just beginning to be understood³. Our gene expression and leaf movement assays have revealed unique phenotypes of *elf4*, which indicate that *ELF4* functions either in a circadian oscillator or by conferring accuracy and persistence on a separate oscillator. Despite a unique role in clock regulation, the effect of *ELF4* on flowering time may occur by a mechanism similar to that of other circadian mutants, that is, through the misexpression of *CO*²¹. Further characterization of the *elf4* mutant will hopefully elucidate how components of the circadian machinery collectively control rhythmic processes throughout the day/night cycle, including the ability of plants to respond to photoperiod. □

Methods

Plant material and growth and conditions

All experiments were carried out on the Ws ecotype. Plants were grown in LD (16 h light/8 h dark) or SD (8 h light/16 h dark) under cool white light (~120 μmol m⁻² s⁻¹) at a constant 22 °C unless indicated otherwise. Hypocotyl-growth assays were done as described²².

Analysis of *ELF4* and *CO* mRNA abundance

We isolated RNA from 1-week-old whole seedlings using TRI reagent (Sigma). Complementary DNA was synthesized by polymerase chain reaction with reverse transcription (RT-PCR) using 5 μg of total RNA, an oligo dT primer with an M13 sequence attached to the 5' end and Superscript II reverse transcriptase (Gibco). As *ELF4* is a single exon gene, RT-PCR was carried out using a gene-specific primer, 5'-TATGAAGA GGAACGGCGAGA-3', and the M13F primer, 5'-GTAAACGACGCCAGTCCC-3', to prevent DNA contamination. *UBQ10* (ref. 23) was amplified as a control. We used 25 and 20 cycles for *ELF4* and *UBQ*, respectively. PCR fragments were transferred to a nylon membrane (Hybond) and hybridized with labelled *ELF4* and *UBQ* cDNAs. We measured *CO* mRNA abundance as described²¹. RNA blots contained 10 μg of total RNA per lane on a denaturing formaldehyde gel (1% agarose). RNA was transferred to a nylon membrane and probed with an *ELF4* antisense RNA probe.

Circadian rhythm assays

The *CAB2-LUC* construction has been described²⁴. The DNA regions immediately upstream of the *CCR2* and *CCA1* genes were amplified by PCR from *Arabidopsis* (Ws-2) genomic DNA. These promoters were fused to luciferase and introduced into *Arabidopsis*. Seeds were stratified (48 h at 4 °C) on Murashige and Skoog (MS) agar medium with 3% sucrose. Seedlings were entrained for 6 d in 12 h light (140 μmol m⁻² s⁻¹ cool white fluorescent light)/12 h dark in controlled environment chambers (Percival or Sanyo) before being introduced into assay conditions²⁴. The luminescence of individual seedlings was measured by low-light video imaging using a liquid nitrogen cooled camera (Roper Scientific)²⁴ or by counting in a Packard Topcount²⁵. Instrument background has been subtracted from the data presented here. Periods were estimated starting from 24 h after the last dark/light transition, using FFT-NLLS software as described²¹. We entrained seedlings for leaf movement assays for 9 d as described above. Leaf growth was monitored by video imaging under LL. Movements of the first primary leaves over the first 90 h of imaging were analysed using FFT-NLLS software as described⁶. Period means and

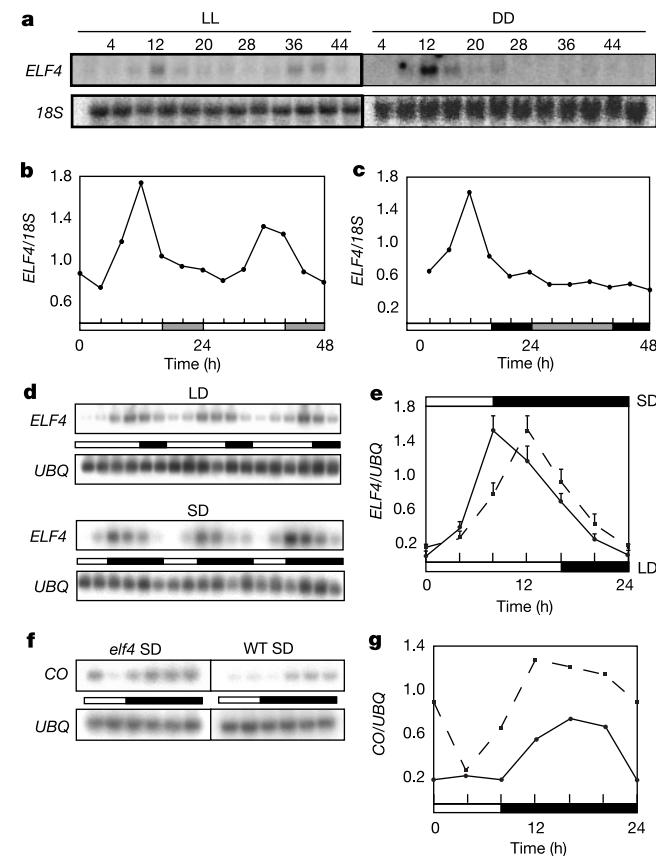


Figure 3 Expression of *ELF4* and *CONSTANS*. **a**, RNA blot of *ELF4* expression in LL and DD. Data are representative of two independent experiments. **b**, **c**, Quantification of *ELF4* expression in LL and DD. White and black rectangles indicate lights on and lights off, respectively. Grey rectangles indicate subjective day and subjective night in **b** and **c**, respectively. **d**, RT-PCR showing *ELF4* expression under LD and SD over 3 d. **e**, Trace showing *ELF4* expression in LD (dashed line) and SD (solid line). Points and error bars indicate the mean ± s.e.m. of three trials for LD and six trials for SD. **f**, RT-PCR showing *CO* expression in SD-grown wild-type (WT) and *elf4*. **g**, Trace showing *CO* expression in wild type (solid line) and *elf4* (dashed line). Data are representative of three independent experiments. The 0-h time point is plotted again at 24 h. White and black rectangles indicate lights on and lights off, respectively.

standard deviations are variance weighted. Rhythmic traces are those with any period estimate in the circadian range, 15–35 h, as described⁸. All rhythm assays were conducted at 22 °C.

Received 9 April; accepted 13 June 2002; doi:10.1038/nature00954.

1. Thomas, B. & Vince-Prue, D. *Photoperiodism in Plants* (Academic, San Diego, 1997).
2. Carré, I. A. Day-length perception and the photoperiodic regulation of flowering in *Arabidopsis*. *J. Biol. Rhythms* **16**, 416–424 (2001).
3. Alabadi, D. *et al.* Reciprocal regulation between *TOC1* and *LHY/CCA1* within the *Arabidopsis* circadian clock. *Science* **293**, 880–883 (2001).
4. Wang, Z. & Tobin, E. M. Constitutive expression of the *CIRCADIAN CLOCK ASSOCIATED 1 (CCA1)* gene disrupts circadian rhythms and suppresses its own expression. *Cell* **93**, 1207–1217 (1998).
5. Putterill, J., Robson, F., Lee, K., Simon, R. & Coupland, G. The *CONSTANS* gene of *Arabidopsis* promotes flowering and encodes a protein showing similarities to zinc finger transcription factors. *Cell* **80**, 847–857 (1995).
6. Koornneef, M., Hanhart, C. J. & van der Veen, J. H. A genetic and physiological analysis of late flowering mutants in *Arabidopsis thaliana*. *Mol. Gen. Genet.* **229**, 57–66 (1991).
7. Samach, A. & Coupland, G. Time measurement and the control of flowering in plants. *BioEssays* **22**, 38–47 (2000).
8. Dowson-Day, M. J. & Millar, A. J. Circadian dysfunction causes aberrant hypocotyl elongation patterns in *Arabidopsis*. *Plant J.* **17**, 63–71 (1999).
9. Hicks, K. A. *et al.* Conditional circadian dysfunction of the *Arabidopsis early-flowering 3* mutant. *Science* **274**, 790–792 (1996).
10. Zagotta, M. T. *et al.* The *Arabidopsis ELF3* gene regulates vegetative photomorphogenesis and the photoperiodic induction of flowering. *Plant J.* **10**, 691–702 (1996).
11. McWatters, H. G., Bastow, R. M., Hall, A. & Millar, A. J. The *ELF3* zeitnehmer regulates light signalling to the circadian clock. *Nature* **408**, 716–720 (2000).
12. Liu, X. L., Covington, M. F., Fankhauser, C., Chory, J. & Wagner, D. R. *ELF3* encodes a circadian clock-regulated nuclear protein that functions in an *Arabidopsis* PHYB signal transduction pathway. *Plant Cell* **13**, 1293–1304 (2001).
13. Covington, M. F. *et al.* *ELF3* modulates resetting of the circadian clock in *Arabidopsis*. *Plant Cell* **13**, 1305–1315 (2001).
14. Hicks, K. A., Albertson, T. M. & Wagner, D. R. *EARLY FLOWERING 3* encodes a novel protein that regulates circadian clock function and flowering in *Arabidopsis*. *Plant Cell* **13**, 1281–1292 (2001).
15. Reed, J. W. *et al.* Independent action of *ELF3* and *phyB* to control hypocotyl elongation and flowering time. *Plant Physiol.* **122**, 1149–1160 (2000).
16. Bell-Pedersen, D., Crosthwaite, S. K., Lakin-Thomas, P. L., Mellow, M. & Okland, M. The Neurospora circadian clock: simple or complex? *Phil. Trans. R. Soc. Lond. B* **356**, 1697–1709 (2001).
17. Aronson, B. D., Johnson, K. A. & Dunlap, J. C. Circadian clock locus frequency: protein encoded by a single open reading frame defines period length and temperature compensation. *Proc. Natl Acad. Sci. USA* **91**, 7683–7687 (1994).
18. Strayer, C. *et al.* Cloning of the *Arabidopsis* clock gene *TOC1*, an autoregulatory response regulator homolog. *Science* **289**, 768–771 (2000).
19. Feldmann, K. A. T-DNA insertion mutagenesis in *Arabidopsis*: mutational spectrum. *Plant J.* **1**, 71–82 (1991).
20. Onouchi, H., Igeno, M. I., Perilleux, C., Graves, K. & Coupland, G. Mutagenesis of plants overexpressing *CONSTANS* demonstrates novel interactions among *Arabidopsis* flowering-time genes. *Plant Cell* **12**, 885–900 (2000).
21. Suarez-Lopez, P. *et al.* *CONSTANS* mediates between the circadian clock and the control of flowering in *Arabidopsis*. *Nature* **410**, 1116–1120 (2001).
22. Davis, S. J., Bhoo, S. H., Durski, A. M., Walker, J. M. & Vierstra, R. D. The heme-oxygenase family required for phytochrome chromophore biosynthesis is necessary for proper photomorphogenesis in higher plants. *Plant Physiol.* **126**, 656–669 (2001).
23. Kardailsky, I. *et al.* Activation tagging of the floral inducer *FT*. *Science* **286**, 1962–1965 (1999).
24. Bognar, L. K. *et al.* The circadian clock controls the expression pattern of the circadian input photoreceptor, phytochrome B. *Proc. Natl Acad. Sci. USA* **96**, 14652–14657 (1999).
25. Carré, I. A. & Kay, S. A. Multiple DNA–protein complexes at a circadian-regulated promoter element. *Plant Cell* **7**, 2039–2051 (1995).

Supplementary Information accompanies the paper on Nature's website (<http://www.nature.com/nature>).

Acknowledgements

This work was supported by the College of Agricultural and Life Sciences of the University of Wisconsin and by a grant to R.A. from the National Science Foundation. M.R.D. was supported by a Molecular Biosciences Training Grant (NIH); R.M.B. was supported by a Gatsby graduate studentship; S.J.D. is a Department of Energy Bioscience fellow of the Life Sciences Research Foundation. Work in Warwick was supported by grants from the Biotechnology and Biological Sciences Research Council and the Human Frontier Science Program (HFSP) to A.J.M. The work in Hungary was supported by the Howard Hughes Medical Institute.

Competing interests statement

The authors declare that they have no competing financial interests.

Correspondence and requests for materials should be addressed to R.M.A. (e-mail: amasino@biochem.wisc.edu) or A.J.M. (e-mail: Andrew.Millar@warwick.ac.uk). The accession code for *ELF4* is AY035183.

.....
Protective role of phospholipid oxidation products in endotoxin-induced tissue damage

Valery N. Bochkov, Alexandra Kadl, Joakim Huber, Florian Gruber, Bernd R. Binder & Norbert Leitinger

Department of Vascular Biology and Thrombosis Research, University of Vienna, Schwarzschanerstrasse 17, 1090 Vienna, Austria; and BMT-Research, Brunnerstrasse 59/5, 1235 Vienna, Austria

Lipopolysaccharide (LPS), an outer-membrane component of Gram-negative bacteria, interacts with LPS-binding protein and CD14, which present LPS to toll-like receptor 4 (refs 1, 2), which activates inflammatory gene expression through nuclear factor κ B (NF κ B) and mitogen-activated protein-kinase signalling^{3,4}. Antibacterial defence involves activation of neutrophils that generate reactive oxygen species capable of killing bacteria⁵; therefore host lipid peroxidation occurs, initiated by enzymes such as NADPH oxidase and myeloperoxidase⁶. Oxidized phospholipids are pro-inflammatory agonists promoting chronic inflammation in atherosclerosis⁷; however, recent data suggest that they can inhibit expression of inflammatory adhesion molecules⁸. Here we show that oxidized phospholipids inhibit LPS-induced but not tumour-necrosis factor- α -induced or interleukin-1 β -induced NF κ B-mediated upregulation of inflammatory genes, by blocking the interaction of LPS with LPS-binding protein and CD14. Moreover, in LPS-injected mice, oxidized phospholipids inhibited inflammation and protected mice from lethal endotoxin shock. Thus, in severe Gram-negative bacterial infection, endogenously formed oxidized phospholipids may function as a negative feedback to blunt innate immune responses. Furthermore, identified chemical structures capable of inhibiting the effects of endotoxins such as LPS could be used for the development of new drugs for treatment of sepsis.

Lipids containing polyunsaturated fatty acids such as 1-palmitoyl-2-arachidonoyl-*sn*-glycero-3-phosphorylcholine (PAPC) are especially prone to oxidative modification. Oxidation of PAPC results in generation of a mixture of oxidation products (OxPAPC), some of which stimulate adhesion of monocytes to endothelial cells and induce expression of inflammatory genes in endothelial cells^{8–10}. Thus, a role for oxidized phospholipids as culprits in chronic inflammation was suggested. On the other hand, we have shown that OxPAPC inhibited neutrophil adhesion to endothelial cells induced by LPS⁸.

Here we show that OxPAPC blocked LPS-induced upregulation of the inflammatory adhesion molecules E-selectin, ICAM-1 and VCAM-1 on human umbilical-vein endothelial cells (HUVEC) (Fig. 1a). The inhibitory effect of OxPAPC was concentration-dependent, with half-maximal inhibition observed at 10 μ g ml⁻¹ OxPAPC (Fig. 1b). The effects of LPS at concentrations as high as 500 ng ml⁻¹ were inhibited by 50 μ g ml⁻¹ OxPAPC. Because expression of E-selectin, ICAM-1 and VCAM-1 is NF κ B-dependent, we examined the influence of OxPAPC on signalling events at different levels of the NF κ B cascade. We found that OxPAPC inhibited LPS-induced activation of a 5 \times NF κ B-luciferase reporter construct (Fig. 1c), binding of p65 to its DNA consensus site (Fig. 1d), and phosphorylation and degradation of I κ B α (Fig. 1e).

NF κ B is activated during inflammation by various receptors including the LPS toll-like receptor 4 (TLR4), the interleukin 1 (IL-1) receptor, and the tumour-necrosis factor- α (TNF α) receptor. In contrast to LPS, TNF α -induced phosphorylation and degra-